Computational Materials Science 88 (2014) 151–155

Contents lists available at ScienceDirect

Computational Materials Science

journal homepage: www.elsevier.com/locate/commatsci

The finite element analysis of the surface transformation hardening process using the power control strategy in order to reduce edge effect problems

Arash Khajeh, Seyed Ahmad Jenabali Jahromi *

Department of Materials Science and Engineering, School of Engineering, Shiraz University, Shiraz 71348-51154, Fars, Iran

ARTICLE INFO

Article history:
Received 31 December 2013
Received in revised form 20 February 2014
Accepted 11 March 2014
Available online 4 April 2014

Keywords:
Finite element analysis
Surface transformation hardening

ABSTRACT

A power control strategy was adopted in the finite element analysis of the surface transformation hardening of S355 steel in order to adjust temperature at the surface of the workpiece in the vicinity of edges. This strategy which is based on controlling the input power of the heat source as a function of the maximum temperature at the surface, allows for gaining a more uniform microstructure as a result of a uniform thermal history at the surface. The results indicate that the applied strategy is highly effective. Besides, the results obtained from the simulations suggest a combination of a large beam size and a high traveling speed in the absence of the proposed approach.

1. Introduction

Surface hardening processes are used to improve the wear resistance of parts without affecting the softer, tough interior bulk materials. This mixture of hard surface and resistance to fracture under impact is beneficial in parts such as a cam or ring gear that must have a very hard surface to resist wear, along with a tough interior to resist the impact that occurs during the operation [1–3]. Although there is a wide variety of techniques which affect the localized regions of the specimen, those employing high energy beams (lasers, electron beams, etc.) as a heat source have a few distinct advantages over the others. In these methods, a high level of energy can be very precisely delivered to a small area of the workpiece [4,5]. Because of the highly localized heated area and high heat conductivity of metals, bulk materials serve as a heat sink and no refrigerant fluid is required [6]. As a result, compared to the regular methods such as flame and induction hardening, surface transformation hardening using high energy beams gives higher heating and cooling rates as well as considerably less thermal distortion [7].

Surface transformation hardening using high energy beams is characterized by several process parameters: the beam power, the traveling speed, the spot dimension, the power distribution and the scanning strategy, especially its trajectory and eventual overlapping degree. All these parameters are strongly correlated to each other and affect the final hardening results [8]. However, Due to high cooling rates in this hardening process, reaching a proper peak temperature for suitable austenization is assumed to be the most essential factor in achieving a desired microstructure [9,10].

Many attempts have been made using analytical [11–21] and numerical [22–30] methods to predict the temperature field and microstructures, which obtained from a moving heat source. However, more attention has been paid to idealized models with restrictions in the heat flow and workpiece dimension. Accordingly, they are not appropriate to assess the edge effects of the workpiece, which tend to concentrate the heat flow. Moreover, the majority of the developed models have been devoted to the studying of the process under quasi-steady state conditions, while a fully time-dependent model is necessary to investigate the thermal behavior of the workpiece under realistic conditions.

The aim of the presented study is to investigate the problems in achieving a uniform microstructure throughout the process in the presence of the edges and complexities of the specimen and to present a solution. For this purpose, the finite element simulation of the process was carried out by the ABAQUS finite element software using both the fixed power and the power control strategy. Finally, the comparison between the results obtained from the two sets of simulations was made to find the optimal process parameters. The application of power control strategy for complex geometry, gives an estimation of required changes of heat source power in practical condition to gain better mechanical properties (wear, pitting and corrosion resistance) as a result of obtaining a more uniform microstructure.

* Corresponding author. Tel.: +98 917 3131535.
E-mail address: Jahromiah@gmail.com (S.A. Jenabali Jahromi).

http://dx.doi.org/10.1016/j.commatsci.2014.03.018
0927-0256/

2. Finite element simulation

2.1. Geometry and mesh model

The modeling of the temperature field in the surface transformation hardening using a moving heat source was performed in the ABAQUS finite element software. Because of the symmetry of the process around the trajectory line, only half of the geometry was modeled. The schematic of the single track process showing the geometric parameters and mesh model has been illustrated in Fig. 1.

The determination of the optimal mesh is essential for the solution of nonlinear governing equations to reduce the analysis time. The finite element mesh, which was refined in the heat affected zone, has been created using the eight-node hexahedral heat transfer elements as shown in Fig. 1. Due to the large temperature gradients, this region is critical for the solution accuracy and convergence [31]. The element's dimensions vary from 0.1 mm in the center of the irradiated region to 5 mm at the farthest locations from this area.

2.2. Thermal analysis model

The transient heat transfer analyses were conducted using 3D models in the ABAQUS/standard commercial finite element software. The transient heat conduction equation in the surface transformation hardening using the moving heat source can be expressed in its most general form as:

$$\rho(T)C_P(T)\left(\frac{\partial T}{\partial t}\right) = \nabla(\lambda(T)\nabla T) + Q \tag{1}$$

where $\rho(T)$, $C_P(T)$ and $\lambda(T)$ denote, respectively, the temperature-dependent density, specific heat and thermal conductivity of the material. The heat source term Q at the right side of Eq. (1) is the internal heat source.

Eq. (1) is completed by the initial condition $t = 0$: $T = T_0$ and the boundary conditions of Drichlet, Neumann, and Newton type, taking into account a heat loss due to convection and radiation [32,33]:

$$-\lambda\frac{\partial T}{\partial n} = -q + \alpha(T|_\Gamma - T_0) + \varepsilon\sigma(T^4 - T_0^4) \tag{2}$$

Here, α is the convective coefficient (assumed as $\alpha = 50\ \mathrm{W\,m^{-2}\,°C^{-1}}$ [34]), ε is the radiation coefficient ($\varepsilon = 0.8$ [35]) and σ is the Stefan–Boltzmann constant ($\sigma = 5.67 \times 10^{-8}\ \mathrm{W\,m^{-2}\,K^{-4}}$). Term $q = q(x, y, 0)$ is the heat flux toward the top surface of the workpiece ($z = 0$) in the source activity zone of the radius r_0 and T_0 is the ambient temperature ($T_0 = 25$ °C).

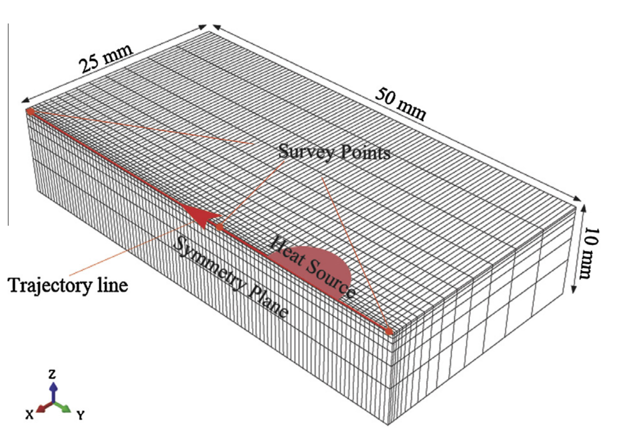

Fig. 1. Schematic of the surface transformation hardening process and dimensions of the modeled geometry.

2.3. Heat source model

In this study, a continuous heat flux with a Gaussian distribution was assumed and applied using the DFLUX user-defined subroutine as follows:

$$q(r,t) = \frac{AP}{r_0^2\pi}\exp\left(-\frac{r^2}{r_0^2}\right) \tag{3}$$

$$r = \sqrt{(x - x_0)^2 + (y - y_0 + vt)^2} \quad 0 \leqslant r \leqslant r_0 \tag{4}$$

where A is the surface absorptivity, P is the heat source power (W), r_0 is the heat source beam radius (m), v is the heat source traveling speed (m/s), x_0 is the initial location of heat source center in the x direction, and y_0 is the initial location of the heat source center in the y direction. In the above equation, $q(x, y, t)$ varies between the maximum heat flux density ($q_{max} = AP/(r_0^2\pi)$) in the center of the heat source and q_{max}/e at $r = r_0$.

2.4. Thermophysical properties

The specimen was assumed to be made of S355 steel with a chemical composition: 0.19 C, 1.05 Mn, 0.2 Si, 0.08 Cr, 0.11 Ni, 0.006 Al, 0.028 P, 0.02 S (wt.%). Thermophysical properties used in the finite element simulations have been summarized in Table 1 [33,36].

2.5. Power control strategy (PCS)

With the aim of reducing the edge effect problems, especially at the start and end of the track, a control strategy for adapting the heat source power based on the maximum temperature at the surface of the model was executed via the DFLUX user-defined subroutine. In addition, the user-defined USDFLD subroutine was employed in order to access the temperature of different points at the surface. In this program, $T_{constant}$ and ΔT have been respectively assigned as constant temperature and acceptable temperature deviation. By means of this method, the temperature of every nodal point in the model can be controlled, regardless of geometry, material properties and process parameters. In this study, $T_{constant}$ was chosen to be 1200 °C which is between Ac3 and melting temperature. The aforementioned trend guarantees the full austenization in the center of the heat source and prevents the surface melting. Fig. 2 shows the sequence of the analysis steps to calculate the temperature field and heat source power.

In order to examine the effectiveness of the PCS, the analyses were repeated with the constant power required to obtain $T_{max} = T_{constant}$ in the middle of the track. Afterward, temperature fields at the extremes of the geometry and in the middle of the track were compared with those related to the power-controlled models. For the purpose of investigating the effects of the process parameters, finite element simulations were conducted utilizing three different traveling speeds (5, 10 and 15 mm/s) and three different heat source radii (2, 4 and 6 mm).

Table 1
The thermophysical properties assumed in the finite element simulations.

Temperature (°C)	Thermal conductivity λ (W/m °C)	Density ρ (kg/m^3)	Specific heat C_p (J/kg °C)
20	52.0	7800	650
200	49.0	7800	650
1000	26.5	7800	650
1477	33.5	7800	650
1502	34.0	7300	745
1527	34.0	6800	840